Nanoscale

Accepted Manuscript

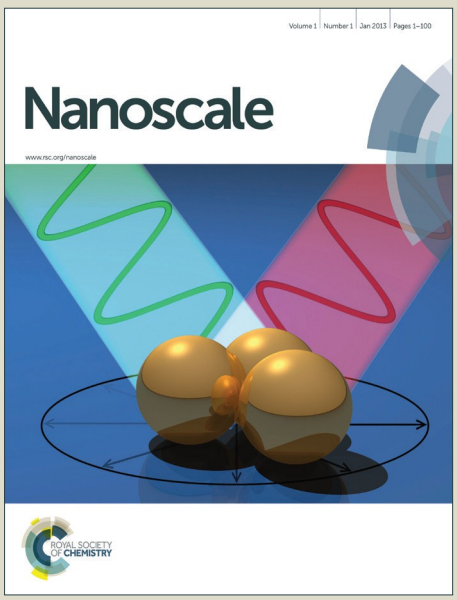

ROYAL SOCIETY OF CHEMISTRY

www.rsc.org/nanoscale

New simple method for Point Contact Andreev Refection (PCAR) using a self-aligned atomic filament in transition-metal oxides

Inrok Hwang[a], *Keundong Lee*[b], *Hyunwoo Jin*[a], *Sunhwa Choi*[c], *Eunok Jung*[c], *Bae Ho Park*[b], *Suyoun Lee*[a,*]

[a]Electronic Materials Research Center, Korea Institute of Science and Technology, Seoul 136-791, Republic of Korea,

[b]Division of Quantum Phases & Devices, Department of Physics, Konkuk University, Seoul 143-701, Republic of Korea

[c]Department of Mathematics, Konkuk University, Seoul 143-701, Republic of Korea

ABSTRACT

Point Contact Andreev Reflection (PCAR) has become a standard method for measuring the spin polarization (*P*) of spintronic materials due to its unique simplicity and the firm physical ground, but it is still challenging to achieve a clean point contact between a superconductor (SC) and a metal (N) for implementing PCAR. In this work, we suggest a much simpler method for the PCAR measurement, where a point contact between SC and N is provided by a metallic filament in a transition-metal oxide generated by electrical bias. This method has been successfully demonstrated using a structure composed of Nb/NiO/Pt, where *P* of the Ni filament was estimated to be about 40 % consistent with the known value of the bulk Ni. In addition, we investigated the dependence of the conductance spectrum on the measurement temperature and the magnetic field. We found that the superconductivity is not fully suppressed until 9 T far above the critical field of Nb, which is associated with the nm-sized constriction of our SC/N junction, much smaller than the coherence length of the SC.

KEYWORDS:

Point Contact Andreev Reflection (PCAR), Resistive Switching, Spin Polarization, Conducting Filament, Superconductor-Metal junction

1. Introduction

Since first introduced for measuring the spin polarization of spintronic materials,[1] PCAR has become a standard method to measure *P* owing to its unique simplicity compared to the other existing methods such as the polarized photoemission[2,3] and the Tedrow-Meservey (TM) method using a tunnel junction between a superconductor and a normal metal.[4,5] It is based on the Andreev Reflection (AR), which is an electron-hole conversion process at the N/SC interface.[6] In AR, the reflected hole should have a spin opposite to that of the incident electron, which allows estimation of the imbalance between the up-spins and down-spins at the Fermi level, i.e. *P*, by measuring the conductance (*G*) of the N/SC interface. The carrier transport in the N/SC structure is well described by a model formulated by G. E. Blonder, M. Tinkham, and T. M. Klapwijk (BTK model) from the ballistic regime to the tunneling regime.[7-10] Due to such a firm quantum mechanical ground, PCAR has also been utilized to study the properties of newly found superconductors, for example, the superconducting proximity effect and the shape of the order parameter of some exotic superconductors.[11,12]

However, the implementation of the PCAR measurement requires a very clean and small N/SC interface in order to keep other mechanisms than the ballistic transport from being involved in and to make the contact resistance high enough to dominate the measured resistance. To date, the PCAR measurement is implemented in mainly two forms. One is to use a SC tip as reported in the original paper, where the contact is formed by moving the tip or the sample. This method is rather simple but the contact is far from being robust. The other is to use an N/SC device with a lithographically defined small constriction. This method has a few variations including a small contact hole obtained by the anisotropic etching of SiN[13,14] and a lithographically defined edge junction.[15] The robustness of the N/SC contact is an

advantage of this method but it requires a rather complex fabrication process, for example, nano-patterning and directional etching processes, which is likely to render a not-so-clean and diffusive N/SC interface.

In this work, we suggest a new method to perform PCAR measurement that is much easier to implement and provides a robust and clean N/SC contact. The contact is formed by a self-aligned metallic filament in a transition-metal oxide which is generated by an electrical bias (a schematic illustration is shown in Figure 1). In binary transition-metal oxides such as NiO_x, TiO_x, and NbO_x, it is well known that a metallic filament is formed electrically by the reduction process, leading to a reproducible resistive switching (RS) phenomenon.[16-19] The size of the metallic filament has been reported to range from sub-nm to a few tens of nm depending on the current passing through the device.[18-20] We investigated the feasibility of this method using Nb/NiO_x/Pt junctions and obtained plausible results showing the typical conductance spectrum of a ballistic N/SC contact.

2. Experiments

Devices composed of Nb/NiO_x/Pt were fabricated as follows. A 130 nm-thick polycrystalline NiO_x thin film was deposited by DC magnetron reactive sputtering on a Pt (100 nm)/Ti/SiO_2/Si substrate. The base pressure was ~ 5×10^{-8} Torr and the working pressure was 1.5 mTorr using Ar(93%) and O_2(7%) gas. The growth temperature was 500 ºC. And then, the top electrode, 100 nm-thick Nb film, was deposited and patterned to have 200 × 200 μm^2 square shape by DC magnetron sputtering and by the conventional lift-off process, respectively.

The resistive switching characteristics of the device were measured by an Agilent 4156B semiconductor parameter analyzer with a conventional probe station system at room temperature. For the PCAR measurement, the DC-current and the differential conductance of a device were simultaneously measured using the standard lock-in technique, where the Keithley 2182 nanovoltmeters, SR830 lock-in amplifier (Stanford Research Inc.), and SR560 low noise voltage amplifier (Stanford Research Inc.) were used. The frequency of ac modulation was 23 Hz. Measurements at low temperature and high magnetic fields were performed using a commercial cryogen-free variable-temperature-insert (VTI) system made by Cryomagnetics Inc.

3. Results and discussion

Figure 2a shows the typical unipolar RS characteristics of a Nb/NiO_x/Pt device at room temperature. In the pristine state, the resistance of the devices is very high. When the applied voltage exceeds the forming voltage ($V_{forming}$~13 V), the current increases abruptly, leading to the low resistance state (LRS). This is so-called the forming process, where a Ni filament is formed by the reduction process. The metallic character of the filament is confirmed by the linearity of the current (I) – voltage (V) curve, as shown in Figure 2b, which is a prerequisite for the PCAR measurement. After the forming process, the switching from the LRS to the high resistive state (HRS) and vice versa occur at the V_{reset}~3 V and V_{set}~6 V, respectively. The superconducting nature of the 100 nm-thick Nb film is confirmed by a sharp drop in the resistance of the Nb film in the device around 9.5 K (see Figure 2c), consistent with the critical temperature of bulk Nb.

For three respective states of the device, i.e. the pristine (Figure 3a), LRS (Figure 3b), and HRS (Figure 3c), the differential conductance was measured as a function of the bias voltage at 1.7 K as shown in Figure 3d. Each state was prepared at room temperature by controlling the applied voltage. The resistance of the device was in the range of 400~500 kΩ (pristine, R_{ini}), 100~200 Ω (LRS, R_L), and 20~30 kΩ (HRS, R_H). The measured resistance consists of a series connection of a few components and we confirmed that the contact resistance between the Nb film and the formed Ni filament was dominant by a calculation of those resistance components (Supplementary Information). For the LRS, note the enhancement of G at low voltage region, which is a signature of the AR, proving the validity of the main idea of this work. Using the Sharvin resistance ($R = \frac{h}{2e^2}\frac{4\pi}{k_F^2 A}$, where R, h, e, k_F, and A are the contact resistance, the Planck constant, the electronic charge of an electron, the Fermi wave vector of Ni, and the contact area, respectively),[14,21] the contact resistance in the LRS gives an estimation of the contact size of 3.4~4.8 nm in diameter with $k_{F,Ni} \sim 0.95$ Å^{-1}.[22] This clearly shows the formation of the very narrow contact. Furthermore, the observed suppression of G for the HRS reminds us of the tunneling conductance spectrum of the N/I/SC junction, where I is an insulator. Considering the absence of the expected peaks around Δ_{sc} (~1.2 meV, the superconducting gap of Nb), the device in the HRS is thought to be in the intermediate region between the tunneling and the diffusive transport regime. Therefore, it seems to imply the possibility of utilizing this method to study the tunneling spectroscopy of the N/I/SC structure as well as the ballistic transport of the N/SC structure by finding optimum preparation conditions.

The observed G-V curve is further analyzed using the aforementioned BTK model modified to include P.[1] The solid line in Figure 4 is the best fitting curve by the modified BTK model

to the observed conductance spectrum, showing a good agreement in the low voltage region. The fitting parameters are P, Z, T and Δ_{sc}, where Z, T, and Δ_{sc} are the value representing the cleanness of the interface with zero for the ballistic contact, temperature, and the superconducting gap of Nb, respectively. For the best fitting, we obtained the values of the fitting parameters, (P, Z, T, Δ_{sc})=(0.4± 0.01, 0.05± 0.01, 3.1 ± 0.1 K, 0.55 ± 0.05 meV) (see Supplementary Information). Note that the obtained P value of 0.4 is consistent with the known values of P of the ferromagnetic Ni obtained by the other methods[1,13,14] verifying the ability of this method for a quantitative analysis. More importantly, we would like to stress that the obtained Z value is almost zero, unequivocally meaning that the carrier transport at the Ni filament-Nb junction is ballistic, a prerequisite for precise determination of P. The calculated temperature ($T_{calc.}$) and $\Delta_{sc.}$ are found to be higher than the measurement temperature ($T_{meas.}$) and lower than that ($\Delta_{sc,Nb}$=1.2 meV) of bulk Nb respectively, which might be associated with the local heating and a proximity-induced superconducting gap at the junction.[13] The deviation from the fitting curve outside ± 2 mV is due to the existence of the broad dip structure in the data. It is not explained within the BTK model but is usually observed around Δ_{sc} in PCAR measurements with a clean interface[1,14,23,24] indicating that the deviation from the BTK model is not caused by the new structure in this work. Nevertheless, the observed dip structure is relatively broader than the typical one obtained by the other methods, and so, it requires further analyses.

Figures 5a and 5b show the temperature- and magnetic field (B)-dependence of the PCAR G-V curve, respectively. Qualitatively, the conductance enhancement due to AR is observed to be suppressed with increasing T and B as the superconductivity of Nb weakens. From the fitting to the modified BTK model, we calculated $T_{calc.}$, Δ_{sc}, and P as a function of T and B. In

Figure 5a, $T_{calc.}$ was found to be higher than the measurement temperature, which might be due to the local heating as mentioned above. We plotted Δ_{sc} as a function of $T_{calc.}$ in the inset of Figure 5a together with a theoretical curve by Bardeen-Cooper-Schrieffer (BCS) model.[25] The origin of the observed discrepancy is unclear at the moment and needs a further analysis. We also plotted Δ_{sc} as a function of B in the inset of Figure 5b. It is interesting to note that the superconductivity is not fully quenched by 9 T, much higher than the upper critical field (H_{c2}) of bulk Nb (H_{c2}~0.45 T).[26,27] This anomalous enhancement of H_{c2} might be associated with the nm-sized scale of our SC/N junction. It is well known that the superconductivity is suppressed by the magnetic field only if the dimension of the specimen is sufficiently larger than the coherence length (ξ_{sc}).[25,28] In our device, the contact area was estimated about 3.4~4.8 nm as mentioned above, much smaller than ξ_{sc} of typical metals (30~2000 nm).[29] This might imply the possibility that the superconductivity in the contact region of our device can survives in such a high magnetic field. In addition, the observations of similar enhancement of H_{c2} were previously reported in the PCAR measurement with a tip-sample configuration[30] and in the superconducting filament.[31]

To generalize this method to probe P of arbitrary spintronic materials, the superconducting filament instead of the metallic one is needed. We tested several Ni/NbO_x/Pt devices aiming at the formation of Nb filament in the NbO_x and obtained the LRS state with the resistance level similar to that of the Nb/NiO_x/Pt device. Nevertheless, we could not observe the enhancement of the differential conductance. We believe that it was due to the unoptimized growth condition of NbO_x and the optimization including the use of other oxides made of superconducting metals such as Ta and Al is under study and will be presented in near future.

4. Conclusions

In summary, a new and simple method for implementing the PCAR measurement is introduced, where a point contact is formed by a self-aligned filament formed during the electrical breakdown in a transition-metal oxide. The idea was verified using Nb/NiO_x/Pt devices, where G in the LRS was observed to be enhanced inside the superconducting gap. The G-V curve was well described by the modified BTK model and gave the estimation of the spin polarization in good agreement with the known value of Ni. The fact that the T- and H-dependence of Δ_{sc} calculated from the fitting to the BTK model follows the BCS theory verifies the dominant role of the AR in determining the conductance of the device. We believe that this new method provides a simple and promising way to implement the PCAR measurement for studying both spintronic and superconducting materials.

ACKNOWLEDGMENT

This research was supported by the KIST Insitutional Program (Project No. 2E25440). K.L. and B.H.P. was supported by the National Research Foundation of Korea (NR F) grant funded by the Korea government (MSIP) (No. 2013R1A3A2042120).

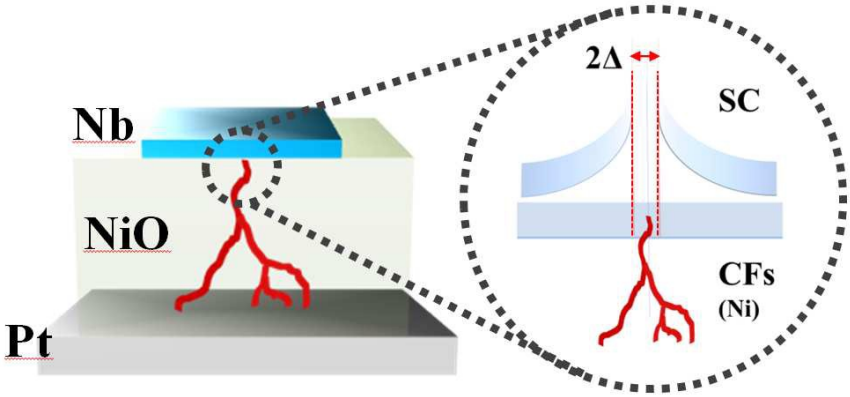

Figure 1. A schematic illustration of the new simple method for the PCAR measurement using a self-aligned metallic filament inside a transition metal oxide formed by the electrical breakdown.

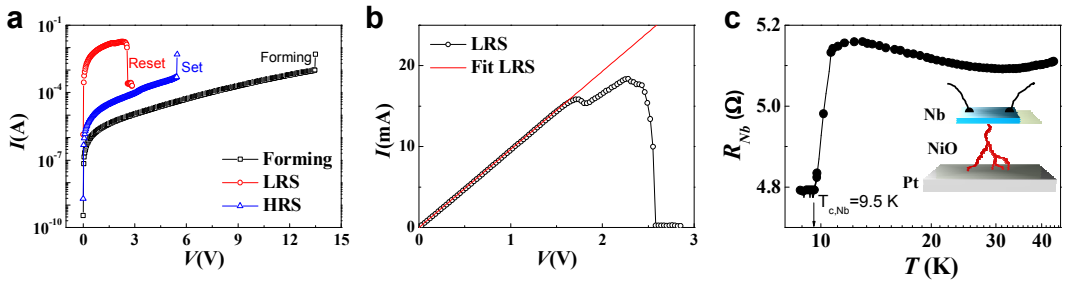

Figure 2. (two-column span) (a) Current (*I*) -Voltage (*V*) curves for unipolar RS (Uni-RS) in a Nb/NiO_x/Pt device in its pristine state (black square), LRS (red circle), and HRS (blue up-triangle), respectively. (b) The linear scale plot of the *I*-*V* curve in the LRS of a device. The solid red line is the linear fitting curve ensuring the formation of Ohmic contact between the Ni filament and Nb. (c) Temperature dependence of the resistance (R_{Nb}) of the Nb film in the device, which was measured by two-probe method as shown in the inset.

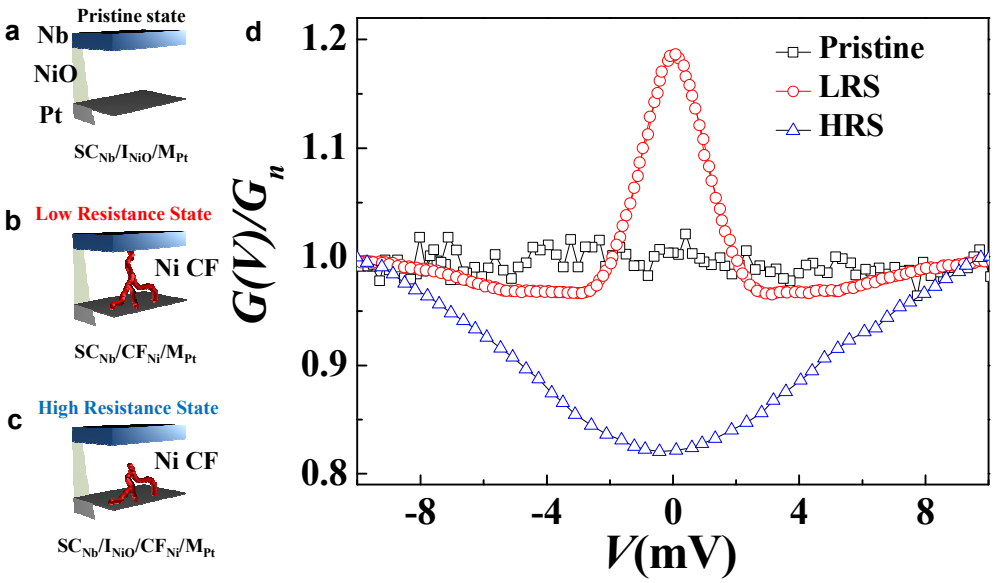

Figure 3. (a)~(c) Schematic illustrations of the pristine state, LRS, and HRS, respectively. (d) Normalized differential conductance ($G(V)/G_n$) as a function of bias voltage (V) for the pristine (black square), LRS (red circle), and HRS (blue up-triangle) at 1.7 K, respectively.

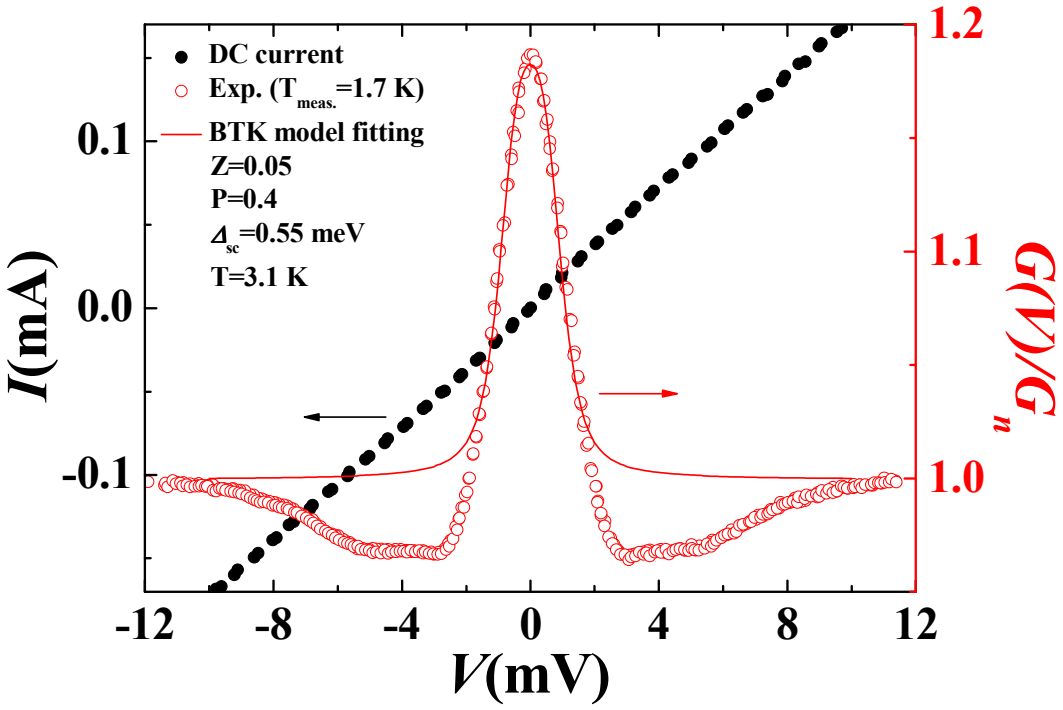

Figure 4. *I-V* (black solid symbol) and *G-V* (red open symbol) curve in the LRS state at 1.7 K. The solid line is the best fitting curve to the modified BTK model, where the fitting parameters are indicated.

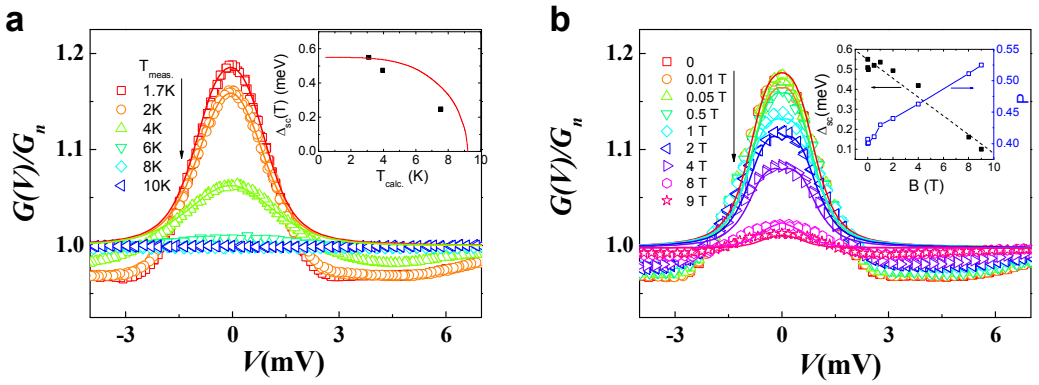

Figure 5. (two-column span) (a) *G*-*V* curves at various temperatures (symbols) and the fitting curves by the BTK model, where $T_{calc.}$ and Δ_{sc} were calculated as fitting parameters with *P* and *Z* fixed at 0.4 and 0.05, respectively. (Inset) Δ_{sc} as a function of $T_{calc.}$. The red solid line is a theoretical curve by BCS model. (b) *B*-dependence of *G*-*V* curve at 1.7 K, where *P* and Δ_{sc} were calculated as fitting parameters with *T* and *Z* fixed at 3.1 K and 0.05, respectively. (Inset) Δ_{sc} (black) as a function of *B*. The black dotted line is a linear fitting to the data. The calculated *P* (blue) is also plotted as a function of *B*. The solid blue line is a guide to the eye.

REFERENCES

1 Soulen, R. J. *et al.* Measuring the Spin Polarization of a Metal with a Superconducting Point Contact. *Science* **282**, 85-88, doi:10.1126/science.282.5386.85 (1998).

2 Feder, R. Polarized Electronic in Surface Physics : Advanced Series in Surface Science. *World Scientific, Singapore* (1985).

3 Jonker, B., Walker, K., Kisker, E., Prinz, G. & Carbone, C. Spin-polarized photoemission study of epitaxial Fe(001) films on Ag(001). *Physical Review Letters* **57**, 142-145, doi:10.1103/PhysRevLett.57.142 (1986).

4 Tedrow, P. & Meservey, R. Spin-Dependent Tunneling into Ferromagnetic Nickel. *Physical Review Letters* **26**, 192-195 (1971).

5 Tedrow, P. & Meservey, R. Spin Polarization of Electrons Tunneling from Films of Fe, Co, Ni, and Gd. *Physical Review B* **7**, 318-326 (1973).

6 Andreev, A. F. Thermal conductivity of the intermediate state of superconductors, Ⅱ *Soviet Physics JETP* **20**, 1490 (1965).

7 Blonder, G., Tinkham, M. & Klapwijk, T. Transition from metallic to tunneling regimes in superconducting microconstrictions: Excess current, charge imbalance, and supercurrent conversion. *Physical Review B* **25**, 4515-4532, doi:10.1103/PhysRevB.25.4515 (1982).

8 Blonder, G. & Tinkham, M. Metallic to tunneling transition in Cu-Nb point contacts. *Physical Review B* **27**, 112-118, doi:10.1103/PhysRevB.27.112 (1983).

9 Octavio, M., Tinkham, M., Blonder, G. & Klapwijk, T. Subharmonic energy-gap structure in superconducting constrictions. *Physical Review B* **27**, 6739-6746, doi:10.1103/PhysRevB.27.6739 (1983).

10 Klapwijk, T. M., Blonder, G. E. & Tinkham, M. Explanation of subharmonic energy gap structure in superconducting contacts. *Physica B+C* **109-110**, 1657-1664 (1982).

11 Szabó, P. *et al.* Evidence for Two Superconducting Energy Gaps in MgB2 by Point-Contact Spectroscopy. *Physical Review Letters* **87**, doi:10.1103/PhysRevLett.87.137005 (2001).

12 Lee, S. *et al.* Measurement of the superconducting gap of MgB2 by point contact spectroscopy. *Physica C* **377**, 202-207 (2002).

13 Upadhyay, S. K., Palanisami, A., Louie, R. N. & Buhrman, R. A. Probing Ferromagnets with Andreev Reflection. *physical Review Letters* **81**, 3247 (1998).

14 Clifford, E. & Coey, J. M. D. Point contact Andreev reflection by nanoindentation of polymethyl methacrylate. *Applied Physics Letters* **89**, 092506, doi:10.1063/1.2345361 (2006).

15 Schmehl, A. *et al.* Epitaxial integration of the highly spin-polarized ferromagnetic semiconductor EuO with silicon and GaN. *Nat Mater* **6**, 882-887, doi:10.1038/nmat2012 (2007).

16 Bruyere, J. C. & Chakraverty, B. K. Switching and negative resistance in thin films of nickel oxide. *Applied Physics Letters* **16**, 40 (1970).

17 Seo, S. *et al.* Reproducible resistance switching in polycrystalline NiO films. *Applied Physics Letters* **85**, 5655, doi:10.1063/1.1831560 (2004).

18 Hwang, I. *et al.* Resistive switching transition induced by a voltage pulse in a Pt/NiO/Pt structure. *Applied Physics Letters* **97**, 052106, doi:10.1063/1.3477953 (2010).

19 Kwon, D. H. *et al.* Atomic structure of conducting nanofilaments in TiO2 resistive switching memory. *Nat Nanotechnol* **5**, 148-153, doi:10.1038/nnano.2009.456 (2010).

20 Kim, K. M. & Hwang, C. S. The conical shape filament growth model in unipolar resistance switching of TiO[sub 2] thin film. *Applied Physics Letters* **94**, 122109, doi:10.1063/1.3108088 (2009).

21 Sharvin, Y. V. On the possible method for studying Fermi surfaces. *Zh. Eksperim. i Teor. Fiz.* **48**, 984-985 (1965).

22 Beth Stearns, M. Simple explanation of tunneling spin-polarization of Fe, Co, Ni and its alloys. *Journal of Magnetism and Magnetic Materials* **5**, 167-171, doi:http://dx.doi.org/10.1016/0304-8853(77)90185-8 (1977).

23 Strijkers, G., Ji, Y., Yang, F., Chien, C. & Byers, J. Andreev reflections at metal/superconductor point contacts: Measurement and analysis. *Physical Review B* **63**, doi:10.1103/PhysRevB.63.104510 (2001).

24 Ji, Y. *et al.* Determination of the Spin Polarization of Half-Metallic CrO_{2} by Point Contact Andreev Reflection. *Physical Review Letters* **86**, 5585-5588, doi:10.1103/PhysRevLett.86.5585 (2001).

25 Tinkham, M. *Introduction to Superconductivity*. (McGraw-Hill, 1996).

26 Kerchner, H. R., Christen, D. K. & Sekula, S. T. Equilibrium properties of the fluxoid lattice in single-crystal niobium. I. Magnetization measurements. *Physical Review B* **21**, 86-101 (1980).

27 Williamson, S. J. Bulk Upper Critical Field of Clean Type-II Superconductors: V and Nb. *Physical Review B* **2**, 3545-3556 (1970).

28 Gennes, P. G. d. *Superconductivity of Metals and Alloys*. (Addison-Wesley, 1966).

29 Kittel, C. *Introduction to Solid State Physics*. 7th edn, (Wiley, 1996).

30 Miyoshi, Y., Bugoslavsky, Y., Minakov, A. A., Blamire, M. G. & Cohen, L. F. Local enhancement of the upper critical field in niobium point contacts. *Superconductor Science and Technology* **18**, 1176-1178, doi:10.1088/0953-2048/18/9/005 (2005).

31 Poza, M. *et al.* Nanosized superconducting constrictions. *Physical Review B* **58**, 11173-11176 (1998).